

Variability of Site Response in Seattle, Washington

by Stephen Hartzell, David Carver, Edward Cranswick, and Arthur Frankel

Abstract Ground motion from local earthquakes and the SHIPS (Seismic Hazards Investigation in Puget Sound) experiment is used to estimate site amplification factors in Seattle. Earthquake and SHIPS records are analyzed by two methods: (1) spectral ratios relative to a nearby site on Tertiary sandstone, and (2) a source/site spectral inversion technique. Our results show site amplifications between 3 and 4 below 5 Hz for West Seattle relative to Tertiary rock. These values are approximately 30% lower than amplification in the Duwamish Valley on artificial fill, but significantly higher than the calculated range of 2 to 2.5 below 5 Hz for the till-covered hills east of downtown Seattle. Although spectral amplitudes are only 30% higher in the Duwamish Valley compared to West Seattle, the duration of long-period ground motion is significantly greater on the artificial fill sites. Using a three-dimensional displacement response spectrum measure that includes the effects of ground-motion duration, values in the Duwamish Valley are 2 to 3 times greater than West Seattle. These calculations and estimates of site response as a function of receiver azimuth point out the importance of trapped surface-wave energy within the shallow, low-velocity, sedimentary layers of the Duwamish Valley. One-dimensional velocity models yield spectral amplification factors close to the observations for till sites east of downtown Seattle and the Duwamish Valley, but underpredict amplifications by a factor of 2 in West Seattle. A two-dimensional finite-difference model does equally well for the till sites and the Duwamish Valley and also yields duration estimates consistent with the observations for the Duwamish Valley. The two-dimensional model, however, still underpredicts amplification in West Seattle by up to a factor of 2. This discrepancy is attributed to 3D effects, including basin-edge-induced surface waves and basin-geometry-focusing effects, caused by the proximity of the Seattle thrust fault and the sediment-filled Seattle basin.

Introduction

The city of Seattle has been designated as one of several metropolitan areas in the United States for urban hazard mapping by the USGS and Federal Emergency Management (FEMA) (Weaver *et al.*, 1999). As part of this effort, seismic hazard maps are being developed by the USGS. This article supports that work with additional measurements of site response. Following the 29 April 1965 (m_b 6.5) Seattle earthquake, the greatest damage was observed in the lower downtown business district in the Duwamish Valley and in West Seattle (Fig. 1) (Mullineaux *et al.*, 1967). The Duwamish Valley is filled with recent alluvium and artificial fill with low shear-wave velocities in the upper 30 m ($V_{30} = 140\text{--}170$ m/sec) (Williams *et al.*, 1999a, 1999b), making the high level of damage not surprising. However, West Seattle is on relatively stiff soils of compacted glacial outwash ($V_{30} = 360\text{--}385$ m/sec), and the damage is harder to explain. Mullineaux *et al.* (1967) states that some residents of West Seattle claim the same area was selectively damaged during the m_b 7.1 1949 earthquake. However, published reports of

the 1949 earthquake do not list West Seattle as an area of heavy damage (Dirlam, 1949; Edwards, 1951). If West Seattle is an area of selective higher amplification of ground motion, its quantification is important for the seismic hazard mapping of the area.

For the purpose of this study, it is useful to divide the surficial geology of the Seattle area into six major units (Fig. 1): (1) Vashon drift glacial outwash deposits of Esperance sand over Lawton clay found in the hills of West Seattle, (2) Vashon drift units including a covering of glacial till in the hills east of downtown Seattle, (3) artificial fill in the Duwamish Valley floor, including Harbor Island and south of downtown, (4) “modified land,” where original surface soil layers have been hydraulically removed, (5) Holocene alluvium, and (6) Tertiary sedimentary rock. From our field deployments we have recorded ground motion on all these units except Holocene alluvium.

King *et al.* (1988) and Carver *et al.* (1998), using the data from three small-magnitude earthquakes, compared the

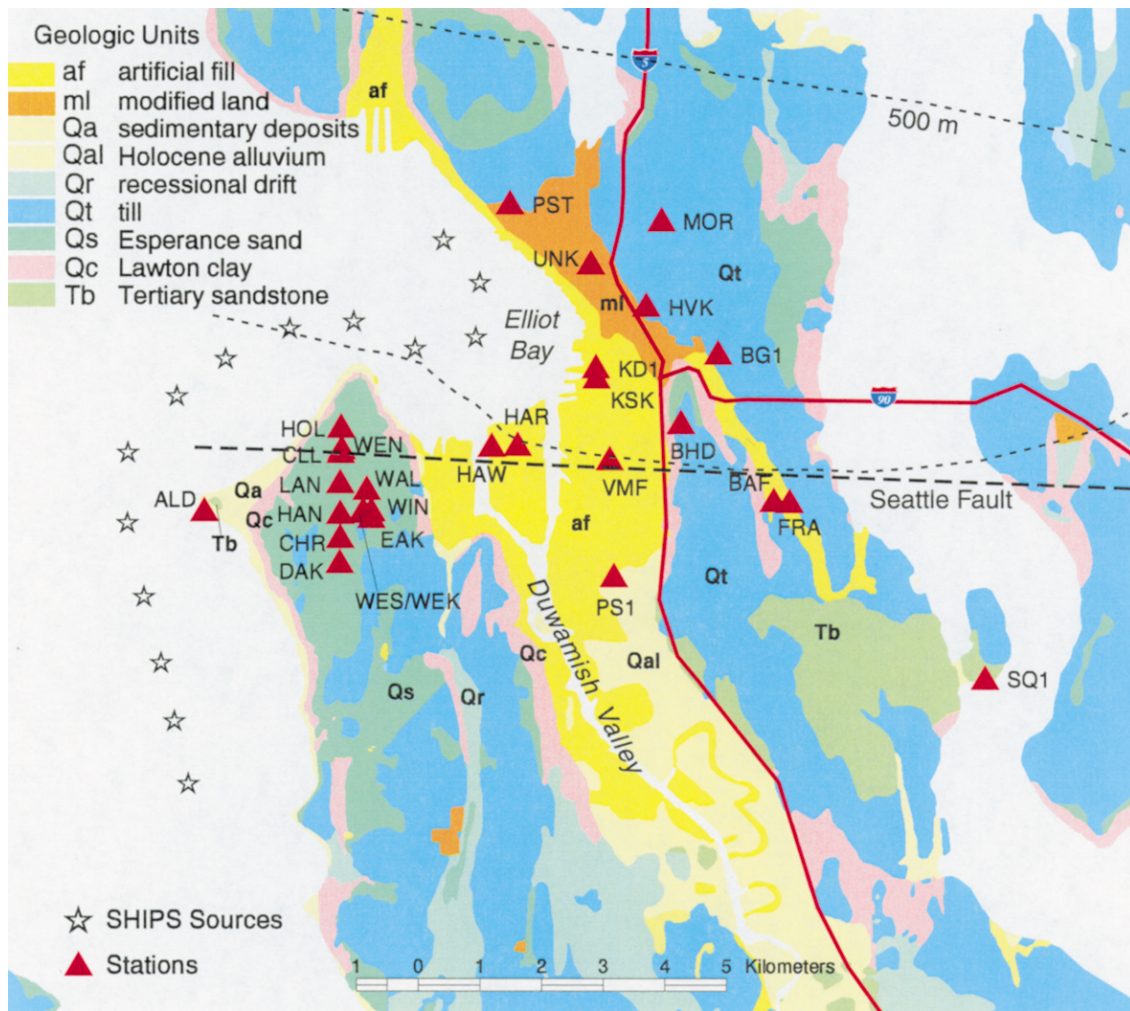


Figure 1. Geologic map of the Seattle area (Liesch *et al.*, 1963) showing locations of earthquake and SHIPS ground-motion recorders listed in Tables 2 and 3. The location of the Seattle fault (Johnson *et al.*, 1994; Pratt *et al.*, 1997) is indicated by the heavy dashed line. The 500-m depth contour of the Seattle basin (Yount *et al.*, 1985) is shown by the light dashed line. West Seattle is the area of high station concentration west of the Duwamish Valley.

ground motion at six sites: one in West Seattle, one on artificial fill on Harbor Island, three on till, and a reference site on sandstone. The West Seattle site gave spectral ratios of approximately 4 in the frequency band 1 to 4 Hz, compared with factors of 2 to 3 for the till sites. Amplification for the Harbor Island site was significantly higher, ranging from 5 to 9 for the same frequency band. Carver *et al.* (1998) concluded that the intensity VIII reported for West Seattle during the 1965 earthquake may be an overestimate and that much of the damage reported to masonry may be due to the use of inferior mortar in construction. Other studies (Langston and Lee, 1983; Ihnen and Hadley, 1986) have used ray tracing techniques to calculate synthetic seismograms and conclude that damage in West Seattle and the Duwamish Valley is consistent with the calculated ground motion if near-surface impedance contrasts are augmented by deeper

basin-geometry-focusing effects. Recently, Frankel *et al.* (1999) calculated site response for different classes of surficial deposits in the Seattle area using weak motions from 21 small-magnitude earthquakes. That study showed large site response in West Seattle, similar to values on artificial fill, with amplifications of 3 to 5 at frequencies of 4 Hz and lower. This article presents site response estimates for nine additional sites in West Seattle. Our results show elevated site response in West Seattle, less than artificial fill sites, but greater than till sites east of Seattle.

Data

Ground-motion data comes from two sources, small-magnitude local earthquakes and airgun shots from the SHIPS experiment (Fisher *et al.*, 1999). To tie our estimates

of site response back to the earlier work of Frankel *et al.* (1999), we consider the same set of earthquake recordings as that study, plus two recent, well-recorded events (2 July 1999 and 3 July 1999). The earthquake data set consists of 23 events, M_L 2.0–5.1, including two mainshock-aftershock sequences, the June 1997 Bremerton sequence, and the February 1997 South Seattle sequence. Table 1 lists the earthquake source information, and Table 2 gives the stations deployed for the recording of earthquake sources. Data from the SHIPS experiment consists of airgun shots around West Seattle in Puget Sound and Elliot Bay (Fig. 1). Forty-five shots were recorded by the West Seattle stations listed in Table 3.

The recording instruments consist of three different types: RefTek PASSCAL recorders with velocity transducers and force-balance accelerometers (FBAs), Kinematics K2s with velocity transducers and FBAs, and Sprengnether DR200s with velocity transducers. The velocity sensors have a natural frequency of 2 Hz and were either Mark Products L-22 or Sprengnether S-6000.

Method of Analysis

The ground-motion data is analyzed in two different ways: spectral ratios and an inversion scheme. The spectral-ratio approach, as used here, has been previously implemented by Hartzell *et al.* (1997). Ground velocity is first calculated by removing the response of the velocity transducer or integration of acceleration records. The records are corrected for a geometrical spreading factor of $1/r$ and the

frequency-dependent attenuation model of Atkinson (1995) for the Pacific Northwest. Our measure of ground motion is the geometric average spectral level within a specified frequency band of the rms of the two horizontal components of ground velocity. The spectra are based on 15 sec of *S*-wave record for the earthquake recordings. For the SHIPS data, record lengths of 10 and 15 sec were used with equivalent results. A reference site is selected for the purpose of calculating relative amplitude ratios. Site amplification is then defined to be the ratio of spectral levels in a given frequency band.

The site-response inversion method we use is based on work originally presented by Andrews (1986), as implemented by Hartzell (1992), Hartzell *et al.* (1996), and Carver and Hartzell (1996). Ground-velocity spectral levels are calculated in the same manner as for the spectral ratio method already discussed. After correcting for path effects and tak-

Table 1
Earthquake Sources Used in This Study

Date (yy/mm/dd)	Time (UTC)	Lat. (N)	Long. (W)	Depth (km)	Mag. (M_L)
96/05/04	14:38	47.76	121.86	7.2	3.3
96/05/05	11:06	47.76	121.86	7.9	3.0
96/06/01	07:22	47.76	121.85	7.2	3.2
96/06/09	14:52	47.75	121.85	5.5	3.0
96/06/19	21:50	47.76	121.85	7.8	3.0
96/06/23	23:37	47.26	122.83	19.3	3.1
96/06/26	19:07	47.76	121.85	4.4	2.6
96/07/03	22:04	47.76	121.88	7.1	3.2
96/09/24	12:45	47.71	122.96	47.3	3.5
96/11/26	05:22	47.71	122.28	23.4	2.7
97/02/10	04:26	47.49	122.34	15	3.5
97/02/10	04:39	47.49	122.34	15	2.0
97/06/23	19:13	47.58	122.56	7.2	4.9
97/06/23	19:16	47.60	122.55	0.5	2.0
97/06/23	19:30	47.60	122.55	1.2	2.6
97/06/23	21:46	47.60	122.55	0.9	3.1
97/06/27	05:30	47.60	122.58	1.5	3.1
97/06/27	09:56	47.58	122.55	1.3	2.5
97/06/27	10:47	47.58	122.55	0.9	3.9
97/06/30	06:07	47.58	122.55	8.4	2.1
97/07/11	01:28	47.58	122.53	6.1	3.5
99/07/02	05:22	47.36	122.38	27.1	3.1
99/07/03	01:43	47.06	123.45	40.7	5.1

Table 2
Earthquake Data Stations

Station	Latitude	Longitude	Surficial Geology
BAF	47.575	122.295	Till
BG1	47.597	122.307	Till
BHD	47.587	122.315	Till
FRA	47.575	122.292	Till
HVK	47.604	122.322	Till
MOR	47.616	122.319	Till
HAR	47.584	122.350	Artificial Fill
HAW	47.584	122.356	Artificial Fill
KD1	47.595	122.333	Artificial Fill
KSK	47.592	122.333	Artificial Fill
PS1	47.565	122.330	Artificial Fill
VMF	47.582	122.330	Artificial Fill
PST	47.619	122.351	Modified Land
UNK	47.610	122.334	Modified Land
EAK	47.574	122.382	Esperance Sand
HAN	47.574	122.388	Esperance Sand
LAN	47.579	122.388	Esperance Sand
WAL	47.578	122.383	Esperance Sand
WEN	47.584	122.388	Esperance Sand
WES (= WEK)	47.574	122.383	Esperance Sand
WIN	47.575	122.382	Esperance Sand
SQ1	47.549	122.250	Sandstone

Table 3
SHIPS Data Stations

Station	Latitude	Longitude	Surficial Geology
CHR	47.571	122.389	Esperance Sand
CLL	47.583	122.388	Esperance Sand
DAK	47.567	122.389	Esperance Sand
EAK	47.574	122.382	Esperance Sand
HAN	47.574	122.388	Esperance Sand
HOL	47.587	122.388	Esperance Sand
LAN	47.579	122.388	Esperance Sand
WEK (= WES)	47.574	122.383	Esperance Sand
WIN	47.575	122.382	Esperance Sand
ALD	47.575	122.418	Sandstone

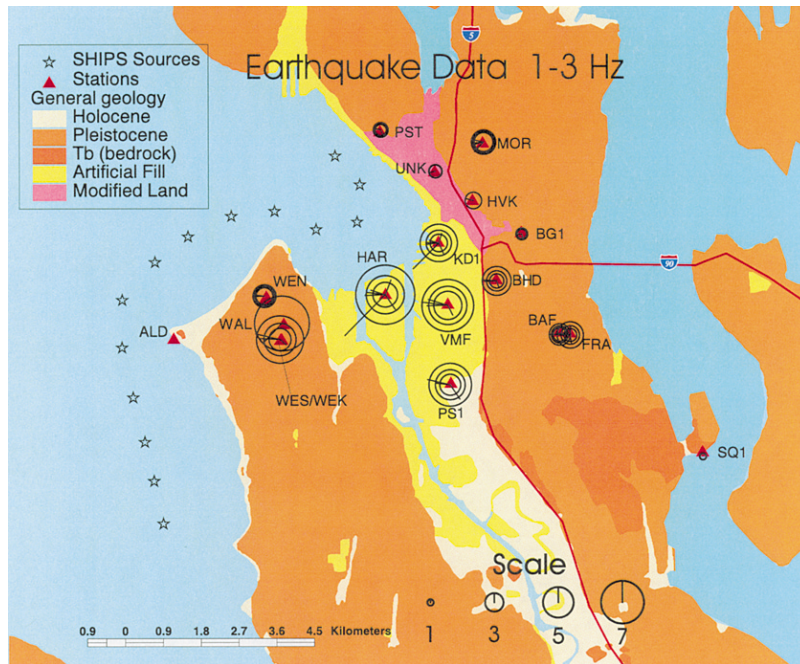


Figure 2. Fourier spectral amplitude ratios based on earthquake data in the frequency band 1–3 Hz. Amplitude ratios are for the rms of the two horizontal components of ground motion and relative to a reference site on Tertiary sandstone at SQ1. See text for explanation of circle and spoke plots at each station.

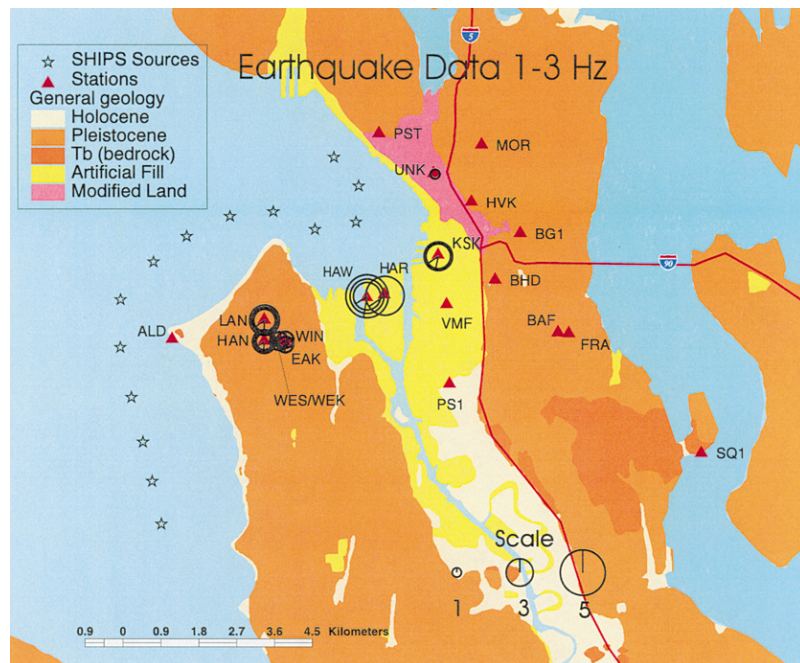


Figure 3. Fourier spectral amplitude ratios in the frequency band 1–3 Hz for two more recent earthquakes (2 July 1999 and 3 July 1999). Amplitude ratios are based on the rms of the two horizontal components of ground motion and relative to a reference site on modified land at UNK. See text for explanation of circle and spoke plots at each station.

ing the logarithm to obtain a linear expression, the data spectrum $U(f)$ may be expressed as the sum of a source term $S(f)$ and a site term $R(f)$, for source i , site j , and frequency k , as

$$\log S_i(f_k) + \log R_j(f_k) = \log U_{ij}(f_k) \quad (1)$$

Equation (1) can be written in matrix form as the least-squares inverse problem

$$\begin{bmatrix} \mathbf{G} \\ \lambda \mathbf{F} \end{bmatrix} \mathbf{x} = \begin{bmatrix} \mathbf{d} \\ \lambda \mathbf{\Gamma} \end{bmatrix}. \quad (2)$$

In this expression, \mathbf{x} is the solution vector of source and site response spectra, \mathbf{d} is the vector of observed ground-motion spectra, \mathbf{G} is a sparse matrix of ones and zeroes indicating the sources and sites for which there is data. The appended equations, $\lambda \mathbf{F} \mathbf{x} = \lambda \mathbf{\Gamma}$, are a constraint needed to remove the undetermined degree of freedom from the problem. λ is a relative weighting factor that balances fitting the constraint against fitting the data. The choice of the constraint is discussed in the results section. Equation (2) is solved using the Chebyshev accelerated tomographic method of Olson (1987). A more detailed discussion of the method is given by Hartzell (1992) and Hartzell *et al.* (1996).

The spectral-ratio results and the inversion results complement each other. With the spectral-ratio approach we are able to calculate relative site amplification for each individual source/station pair, and thereby evaluate azimuthal variations. The strength of the inversion method lies in its ability to utilize all the data, regardless of whether a particular event is recorded at the chosen reference site, to obtain average site response values.

Site-Response Results

Earthquake Data

Figure 2 summarizes spectral-ratio results in the frequency band 1–3 Hz for the earthquake data set in common with the study of Frankel *et al.* (1999). The reference site is SQ1 (Bailey Peninsula, Tertiary sandstone). The results are presented as a series of circles and spokes. Each station is given three concentric circles. All circle sizes are relative to the reference circle at SQ1 with unit radius. The radius of the middle circle is proportional to the geometric mean of the site amplification, averaged over all events recorded at that station. The radii of the outer and inner circles are equal to the geometric mean multiplied by and divided by, respectively, the geometric deviation. The length of each spoke is proportional to the amplification for each individual earthquake. The azimuth of the spoke gives the backazimuth to the source.

Spectral ratio site amplification values are given in Table 4 for the two frequency bands, 1–3 Hz and 3–5 Hz. Sites on artificial fill (HAR, KD1, VMF, PS1) show on average the highest amplification values, consistent with their low

Table 4
Amplification Factors from Spectral Ratios: Earthquake Data, Reference Site SQ1

Station	Mean (1–3 Hz, 3–5 Hz)	Standard Deviation (1–3 Hz, 3–5 Hz)	Num. of Sources
BAF	2.78, 1.36	1.27, 1.05	2
BG1	1.71, 1.26	1.14, 1.20	5
BHD	3.34, 1.67	1.43, 1.51	7
FRA	3.03, 1.62	1.43, 1.36	7
HVK	2.72, 1.00	—	1
MOR	3.55, 2.16	1.14, 1.36	7
HAR	6.35, 4.34	1.55, 1.66	9
KD1	4.21, 1.54	1.47, 1.71	10
PS1	4.95, 2.95	1.43, 1.40	6
VMF	6.34, 3.49	1.36, 1.47	6
PST	2.11, 1.37	1.17, 1.53	2
UNK	2.14, 1.89	1.04, 1.42	3
WAL	9.09, 3.37	—	1
WEN	3.25, 2.79	1.17, 1.15	3
WES	5.32, 3.19	1.47, 1.25	6

average V_{30} of 145 m/sec (Williams *et al.*, 1999a, 1999b). As pointed out by Frankel *et al.* (1999), these sites can also display resonance peaks from low-velocity surface layers of artificial fill and younger alluvium over stiffer soil. As an example, the higher amplification at KD1 in the 1–3 Hz band, compared to the 3–5 Hz band, is due to a prominent resonance peak at 2 Hz. Sites on the hills of Seattle (FRA, BAF, BHD, BG1, HVK, MOR) lie on Pleistocene-age deposits of mainly glacial till. These stiff-soil sites show significantly lower site amplification than the fill sites, and have higher V_{30} values of 390 to 680 m/sec (Williams *et al.*, 1999a, 1999b). Resonances at these sites are not common. The two sites on modified land (UNK, PST) also have low amplifications. The three West Seattle sites (WAL, WEN, WES) have unexpectedly large amplifications, given the stiff-soil conditions and moderately high V_{30} values of 360 to 385 m/sec. The West Seattle sites are all on glacial outwash deposits of Esperance sand over Lawton clay. The only apparent difference between sites on the hills east of downtown and in West Seattle that is evident at the surface is a layer of glacial till east of downtown. Till thickness is variable, but generally not more than 10-m thick (Galster and Laprade, 1991). One earthquake near Olympia with a back-azimuth of 225 degrees gives particularly large amplification factors at WAL, HAR, and KD1 for the 1–3 Hz frequency band. This event contributes to the large deviation about the mean for these stations and points out the need for additional estimates of site response.

From Table 4 the average amplification factors in the frequency band 1–3 Hz for each surficial geologic unit relative to SQ1 are 2.1 (modified land), 2.8 (till), 4.2 (Esperance sand, West Seattle), and 5.4 (artificial fill). We have omitted the value at WAL from the Esperance sand average because this site recorded only one source with an anomalous amplitude. From these data, the response of West Seattle is intermediate to that of the till sites on the hills east of down-

town Seattle and the artificial fill sites in the Duwamish Valley. Table 5 and Figure 3 give amplification factors based on spectral ratios of ground motion from the two more recent earthquakes on 2 July 1999 and 3 July 1999. Because we do not have a sandstone reference site for these events, site UNK on modified land is used as the reference. Using our estimated amplification factor of approximately two for UNK relative to sandstone, yields amplification factors for West Seattle (EAK, HAN, LAN, WEK, WIN) and artificial fill (HAR, HAW, KSK) consistent with the above average values.

In addition to spectral amplitudes, the duration of ground motion is an important parameter in evaluating earthquake hazard. Figure 4 shows representative ground-velocity records filtered from 0.5 to 2.0 Hz for the earthquake on 2 July 1999. The artificial fill site HAW clearly shows a significantly longer duration of motion than the sites in West Seattle (EAK, HAN, WEK, WIN, LAN) and on modified land (UNK). KSK, although on artificial fill, is on the edge of the Duwamish Valley and does not have as thick an accumulation of low-velocity material. To give a quantitative measure of the duration effects, we use the 3D response spectrum calculation of Safak (1998). This approach incorporates duration in response spectra by taking into account the secondary peaks, as well as the largest peak, of the displacement response of a single-degree-of-freedom oscillator. A 3D response spectrum is a surface representing the peak displacements of the oscillator as a function of period and the number of crossings. The 3D response-spectrum intensity is defined to be the area under this surface. Figure 5 plots displacement, velocity, and acceleration 3D response-spectrum-intensity values for two different earthquakes. Event 2 July 1999 compares these values for the records shown in Figure 4. The greatest difference between the West Seattle, artificial fill, and modified land sites is seen in the longer-period displacement response-spectrum intensities. Although the spectral amplitudes show only a 30% increase in going from West Seattle to artificial fill sites, there is up to a factor of 3 greater displacement response-spectrum intensity on artificial fill. The differences between these stations is less for the velocity and acceleration response-spectrum intensity measures. These results are consistent with the trapping of surface-wave energy within the low-velocity sediments of the Duwamish Valley. Event 11 July 1997 in Figure 5 compares east Seattle till sites (BHD, MOR) and Tertiary sandstone (SQ1) with West Seattle (WEN) and artificial fill sites (HAR, KD1, VMF). The till sites are lower in intensity by up to a factor of 2 compared to West Seattle.

The site-response inversion method was also applied to the earthquake data set. To use this method, a constraint on the solution must be specified. This constraint usually takes the form of specifying the site response at one station or the average response of a group of stations. Hartzell (1992), Hartzell *et al.* (1996), and Carver and Hartzell (1996) all constrained the solution by fixing the amplification at a

Table 5
Amplification Factors from Spectral Ratios: Earthquake Data, Reference Site UNK

Station	Mean (1-3 Hz, 3-5 Hz)	Standard Deviation (1-3 Hz, 3-5 Hz)	Num. of Sources
HAR	4.29, 4.18	—	1
HAW	3.79, 2.74	1.25, 1.25	2
KSK	2.94, 1.58	1.08, 1.13	2
EAK	1.75, 1.63	1.04, 1.21	2
HAN	2.15, 2.15	1.21, 1.04	2
LAN	2.81, 2.91	1.18, 1.63	2
WEK	1.98, 1.85	1.03, 1.16	2
WIN	1.81, 1.51	1.03, 1.21	2

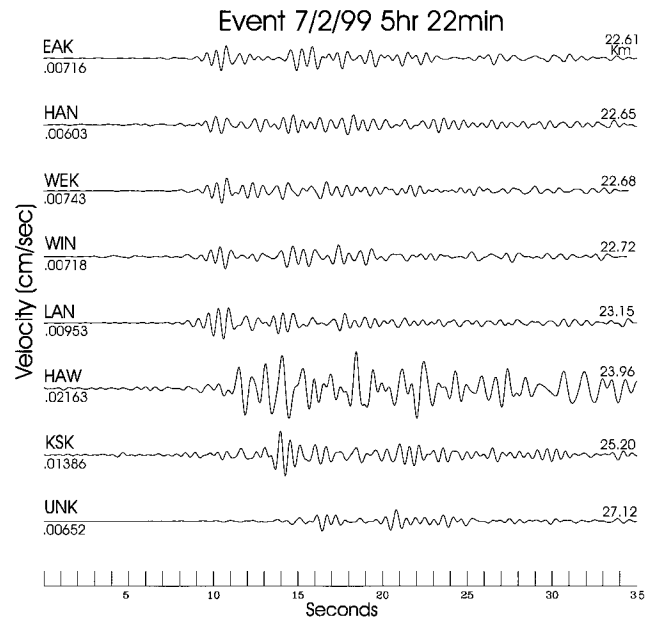


Figure 4. Transverse-component velocity records for the magnitude 3.1 earthquake on 2 July 1999, north of Tacoma, Washington, filtered from 0.5 to 2.0 Hz. Figure compares ground motion at West Seattle sites (EAK, HAN, WEK, WIN, LAN), Duwamish Valley fill sites (HAW, KSK), and a modified land site (UNK). The epicentral distance is given in kilometers.

rock site to 1.0. For the earthquake data set, the site SQ1 on sandstone has the lowest response, and is a logical choice for the constraint site. However, Frankel *et al.* (1999) obtained a response somewhat different from 1.0 for SQ1. To compare with their results we used their calculated site response for SQ1 as our constraint. Figure 6 compares the results of the two studies at selected stations on different surficial geology. The good agreement verifies the consistency of the two approaches, even though very different assumptions and analytical methods are used. Equation (1) makes no assumption about the shape of the source spectra and leads to a linear problem. The method of Frankel *et al.* (1999) assumes ω^{-2} source spectra and is solved by a non-

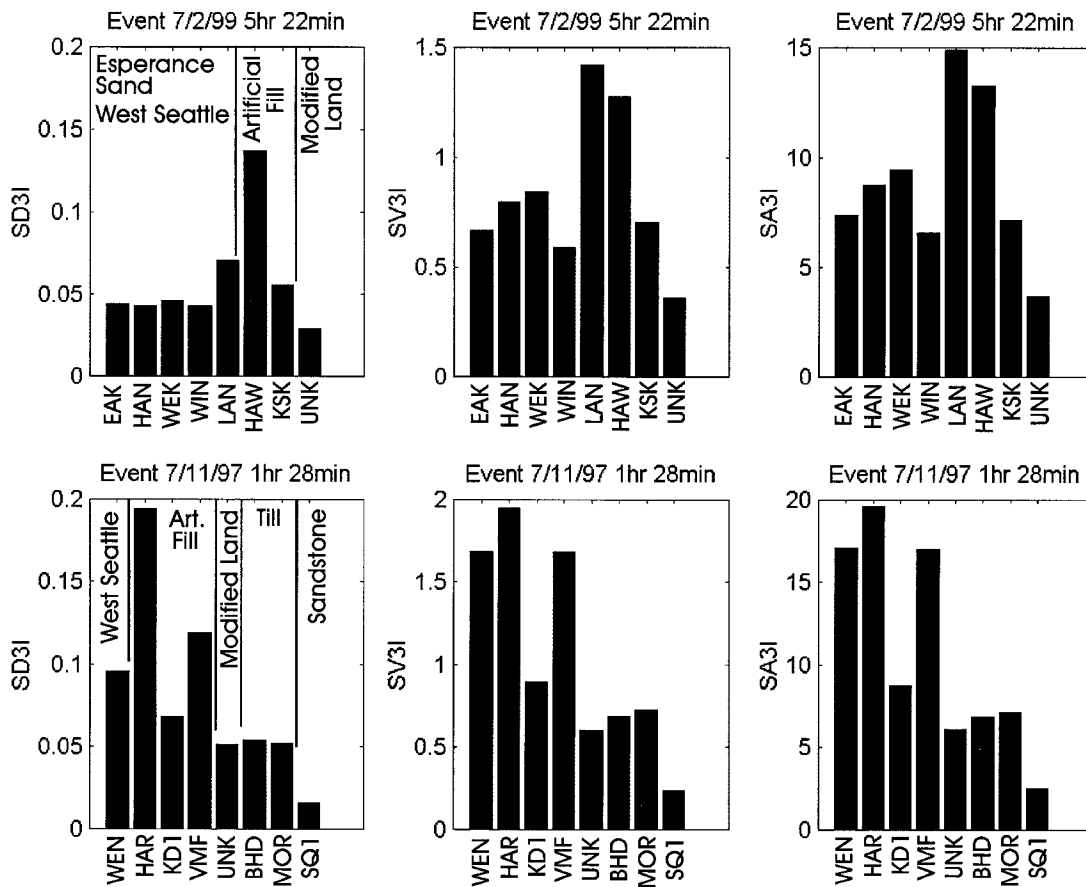


Figure 5. 3D response-spectral intensity values for displacement (SD3I), velocity (SV3I), and acceleration (SA3I). Frames compare West Seattle sites (EAK, HAN, WEK, WEN, WIN, LAN), fill sites (HAW, HAR, KSK, KD1, VMF), modified land (UNK), till sites (BHD, MOR), and Tertiary sandstone (SQ1).

linear analysis. The amplitude of 4 for the 2 Hz spectral peak at site KD1 is more consistent with the theoretically estimated response at this location from drill hole velocity measurements, than the amplitude of 3 from the Frankel *et al.* (1999) study.

The inversion method was also used to calculate the azimuthal variation in site response. This calculation is done by successively rotating the two horizontal components of ground motion into different angles clockwise from north. The site-response inversion is performed for each of these rotations and the results saved. Contour maps of site response versus frequency and azimuth can then be made. For this calculation it is important to use a site as a reference which has negligible azimuthal dependence in its response. Any azimuthal dependence of the reference site will be mapped into all other sites. The low-amplitude till site, BG1, meets this requirement and is used as the constraint site for our azimuthal calculations. Figure 7 shows the results for the two stations with the most prominent azimuthal dependence (HAR, PS1). Both stations are on artificial fill in the Duwamish Valley. They have strong peaks in response at 50 and 90 degrees clockwise from north, respectively. These

angles suggest preferential propagation of waves in the direction of the short axis of the Duwamish Valley and are consistent with our earlier interpretation of trapped surface wave energy and longer duration records at the artificial fill sites. The smaller angle at HAR may be due to the opening up of the Duwamish Valley into Elliot Bay.

SHIPS Data

Figure 8 shows representative horizontal time-domain records from the West Seattle array of stations for one airgun shot. The records are aligned on the first arrival. Although it is difficult to pick *S* waves, comparing vertical and horizontal components shows that the horizontal components are primarily shear waves. Very similar results were obtained using the entire horizontal record and by first removing the theoretical *S-P* delay time from the horizontal components. Station ALD (Alki Point) is on Tertiary sandstone near sea level (Fig. 2), the same unit as site SQ1. The remaining stations are at an elevation of approximately 80 m. The relief of West Seattle is made up of compacted glacial outwash deposits of mainly sands and clays (Mullineaux *et al.*, 1967; Yount *et al.*, 1985). The larger amplitude and longer dura-

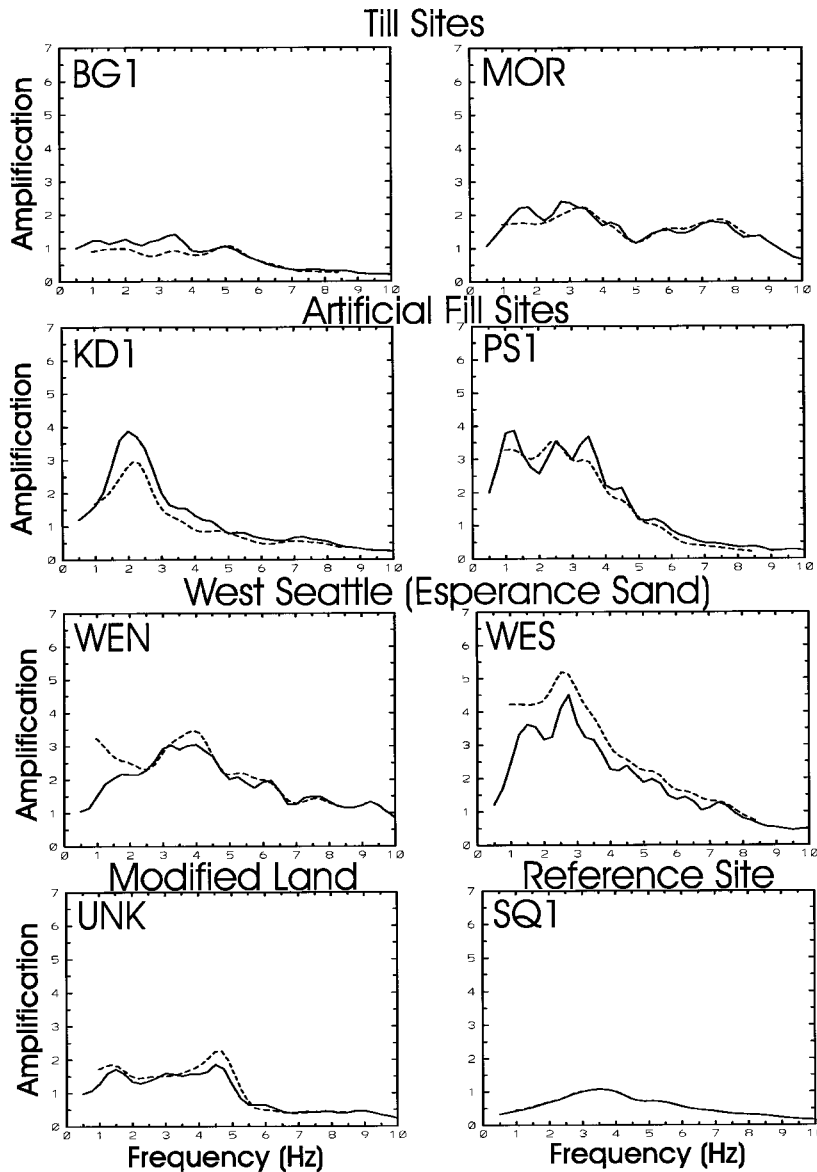


Figure 6. Comparison of site response spectra by the inversion method from this study (solid line) and Frankel *et al.* (1999) (dashed line). Both calculations use the same reference response at SQ1.

tion ground motion at West Seattle sites, relative to ALD, is clear.

An inversion of the SHIPS ground-motion data was performed, using the constraint that the site response at ALD (Tertiary sandstone) is 1.0 for all frequencies, with a kappa value of $\kappa = 0.03$ (Anderson and Hough, 1984). Although there is no constraint in the inversion on the source spectra, we know in this case that all the sources should be similar. Figure 9 shows the mean of all the source spectra and the standard deviation of the mean. The source spectra are very consistent. Figure 9 also points out a weakness of the SHIPS ground-motion data that was not apparent before the study began. Below about 5 Hz the source spectral amplitudes fall off rapidly. Low-pass filtering of the time-domain records reveals that below 5 Hz the SHIPS signal is below the background noise level. Therefore, below 5 Hz the SHIPS spectral

ratios and inversion results are based on ambient noise spectra. Because of this limitation in the data, we do not use the SHIPS results below 5 Hz, other than to point out an interesting agreement between the site response obtained at a common site to the SHIPS data set (WEK) and the earthquake ground motion data set (WES) in West Seattle (Fig. 2). Figure 10 compares the site-response curves obtained from the inversion of the two data sets. The curves are similar. Field and Jacob (1993) present theoretical support for the use of ambient noise in the estimation of site response. Field *et al.* (1990) found microtremors to be useful in determining resonant peaks. However, ambient noise has generally only been found to yield useful information on site response when taking the ratio of horizontal to vertical spectra (Field *et al.*, 1995; Bodin and Horton, 1999), by the method of Nakamura (1989). The problem with using ambient noise in other site

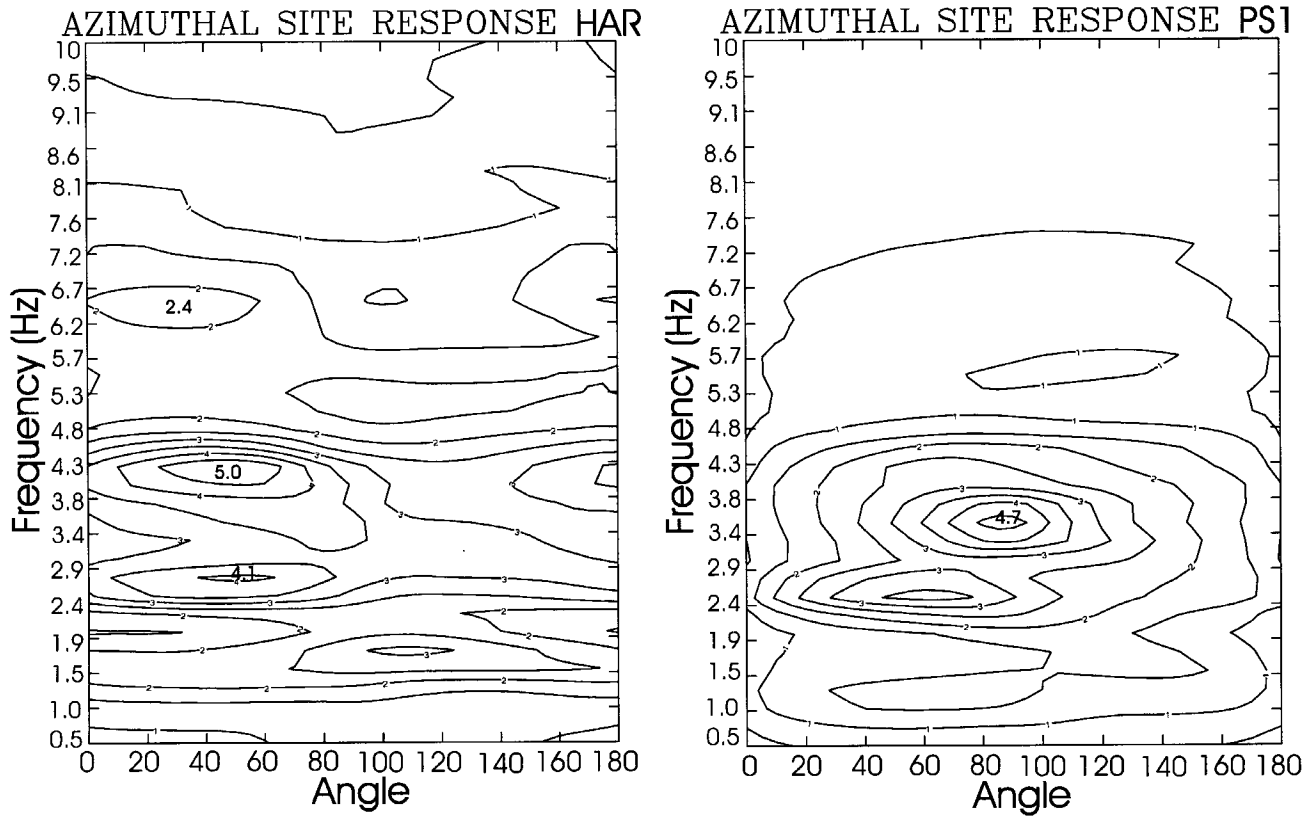


Figure 7. Azimuthal dependence of site response obtained by rotation of horizontal components into different angles measured clockwise from north. Duwamish Valley sites, HAR and PS1, show the greatest preferential directions of motion at, respectively, 50 and 90 degrees clockwise from north.

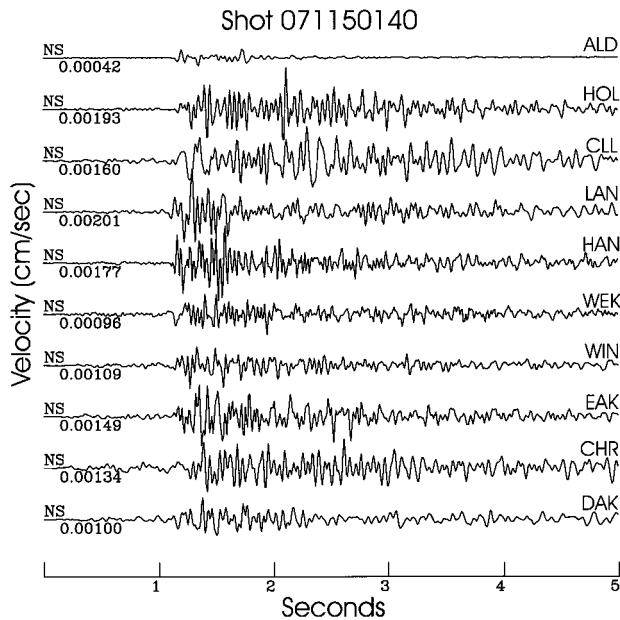


Figure 8. North-south component of ground motion for one SHIPS airgun source recorded across the West Seattle array of stations. ALD is located on Tertiary sandstone. The remaining stations are on a sequence of till, Esperance sand, Lawton clay, and non-glacial sediment.

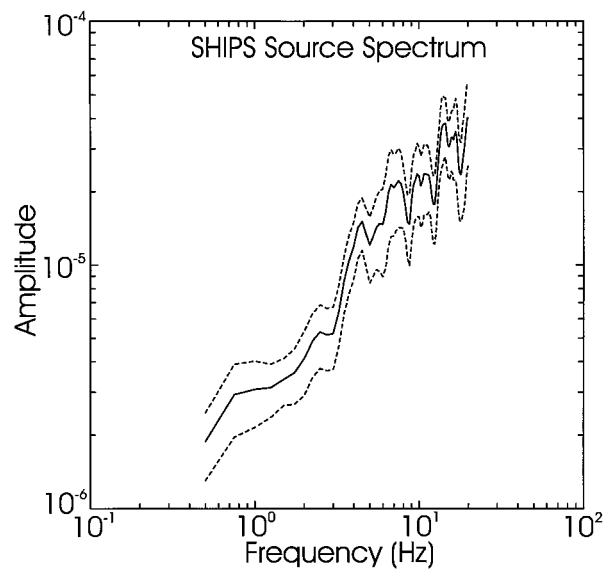


Figure 9. The mean (solid line) and plus and minus the standard deviation (dashed lines) of the SHIPS source spectra from the source/site inversion.

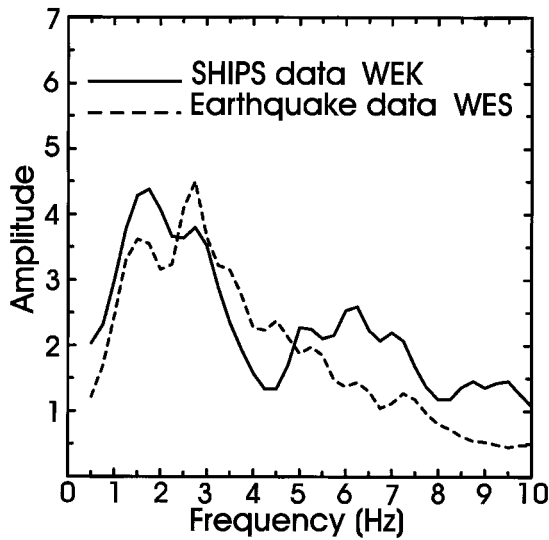


Figure 10. Comparison of site response at the common location WES (earthquake) and WEK (SHIPS) from two separate source/site inversions, one based on earthquake data and one based on SHIPS data.

response calculations such as ours is related to the difficulty of defining the same input sources at reference and nonreference sites. The results in Figure 10 are intriguing but difficult to substantiate.

Figure 11 shows circle and spoke spectral-ratio plots for the SHIPS data in the frequency range 5 to 7 Hz, where there

is a good signal-to-noise ratio. The reference station for these ratios is ALD. Although the SHIPS sources extend clockwise from the southwest to the northeast of West Seattle, an instrumentation problem at ALD limited the recording of both horizontal components to a more restricted range of back-azimuths, primarily to the north. Figure 11 is based on all sources for which the rms of the two horizontal components could be calculated. All stations show significant amplification relative to ALD. Mean values and standard deviations are given in Table 6. The average amplification for all the sites is 5.8. It is difficult to compare these values on an absolute scale with the spectral-amplitude ratios from the earthquake data set (Tables 4 and 5) because they are based on a different reference site. Although ALD and SQ1 are both mapped as Tertiary sandstone, ALD has a significantly higher V_{30} value of 1190 m/sec compared with 433 m/sec for SQ1 (Williams *et al.*, 1999a, 1999b). No earthquakes have been recorded at ALD.

Modeling

Given our observations, we wish to determine what aspects of the ground-motion amplification pattern are predictable using simple models of the velocity structure. From the geologic compilation work of Waldron *et al.* (1962), Liesch *et al.* (1963), and Yount *et al.* (1985), tunnel borings in West Seattle (HDR Engineering and Converse Consultants, unpublished report, 1993), and local shear-wave velocity measurements of Williams *et al.* (1999a, 1999b) and

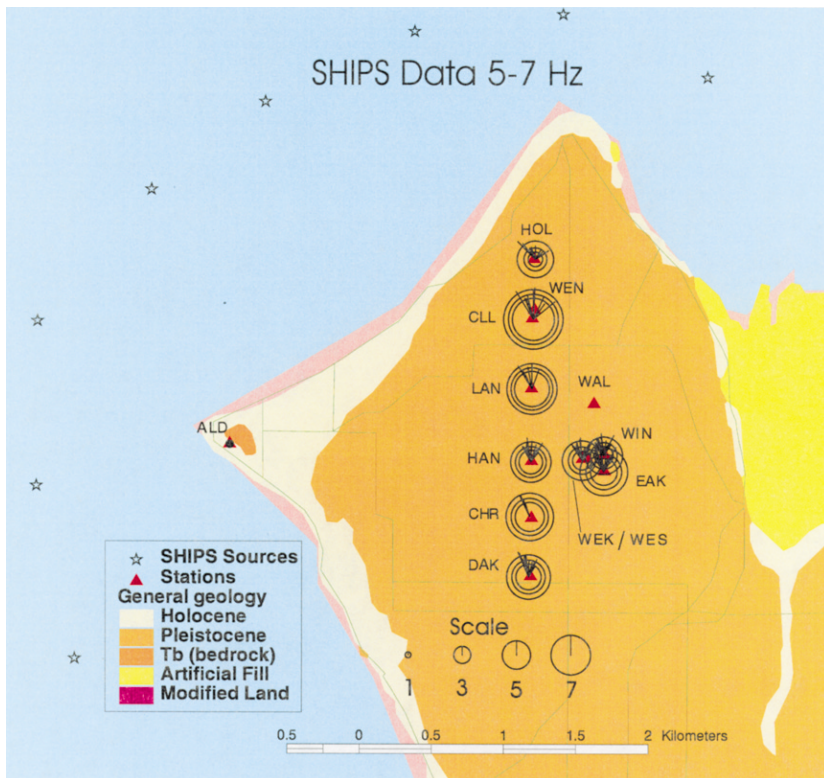


Figure 11. Fourier spectral-amplitude ratios based on SHIPS data in the frequency band 5–7 Hz. Amplitude ratios are for the rms of the two horizontal components of ground motion and relative to a reference site on Tertiary sandstone at ALD. Stars show the location of a few of the SHIPS sources to indicate the general path taken by the ship. See text for explanation of circle and spoke plots at each station.

Shannon and Wilson (1994), we can estimate shallow velocity models. We have adopted the following shear-wave velocities for the primary geologic units: artificial fill (100 m/sec), Holocene alluvium (250 m/sec), near-surface till (350 m/sec), buried till (700 m/sec), near-surface Esperance sand (300 m/sec), buried Esperance sand (410 m/sec), Lawton clay (450 m/sec), nonglacial sediments (600 m/sec), and Tertiary sandstone (1225 m/sec). The term nonglacial sediments refers to deposits from interglacial periods of primarily sand and gravel. One datum we wish to compare with is the difference in amplification factors for shear waves between West Seattle and the hills east of downtown, which we will refer to as east Seattle. Tables 7 and 8 show our

estimates of 1D SH velocity structures for east and West Seattle. The hills of West Seattle are composed of units of the Vashon drift glacial outwash sequence of Esperance sand over Lawton clay. Beneath these units are nonglacial sediments over Tertiary sandstone (bedrock). Borings associated with tunnel construction in West Seattle (HDR Engineering and Converse Consultants, unpublished report, 1993) show the sand and clay units to be highly variable in thickness, but do not give the basement depth. A minimum depth can be estimated of about 120 m. Yount *et al.* (1985) obtained a shallower basement depth of 79 m based on other borehole data. Varying the thickness of our layers over this range shifts resonance peaks but does not significantly affect am-

Table 6
Amplification Factors from Spectral Ratios: SHIPS Data, Reference Site ALD

Station	Mean (5-7 Hz)	Standard Deviation (5-7 Hz)	Num. of Sources
CHR	6.59	1.28	4
CLL	8.86	1.19	9
DAK	5.90	1.32	15
EAK	6.29	1.34	21
HAN	5.46	1.31	20
HOL	4.03	1.60	13
LAN	7.43	1.20	6
WEK	4.80	1.45	22
WIN	4.65	1.42	22

Table 7
Velocity Model for 1D West Seattle Structure

Layer	Thickness (m)	Shear Velocity (m/sec)	Density (g/cm ³)
Near-Surface Esperance Sand	10.0	300.0	1.95
Esperance Sand	20.0	410.0	2.10
Lawton Clay	20.0	450.0	2.15
Non-glacial Sediment	30.0	600.0	2.20
Sandstone	—	1225.0	2.30

Table 8
Velocity Model for 1D East Seattle Structure

Layer	Thickness (m)	Shear Velocity (m/sec)	Density (g/cm ³)
Near-Surface Till	5.0	350.0	1.95
Till	10.0	700.0	2.00
Esperance Sand	20.0	410.0	2.10
Lawton Clay	20.0	450.0	2.15
Nonglacial Sediment	100.0	600.0	2.20
Nonglacial	100.0	650.0	2.20
Nonglacial	100.0	700.0	2.20
Nonglacial	100.0	750.0	2.20
Nonglacial	100.0	850.0	2.20
Nonglacial	100.0	950.0	2.20
Sandstone	—	1225.0	2.30

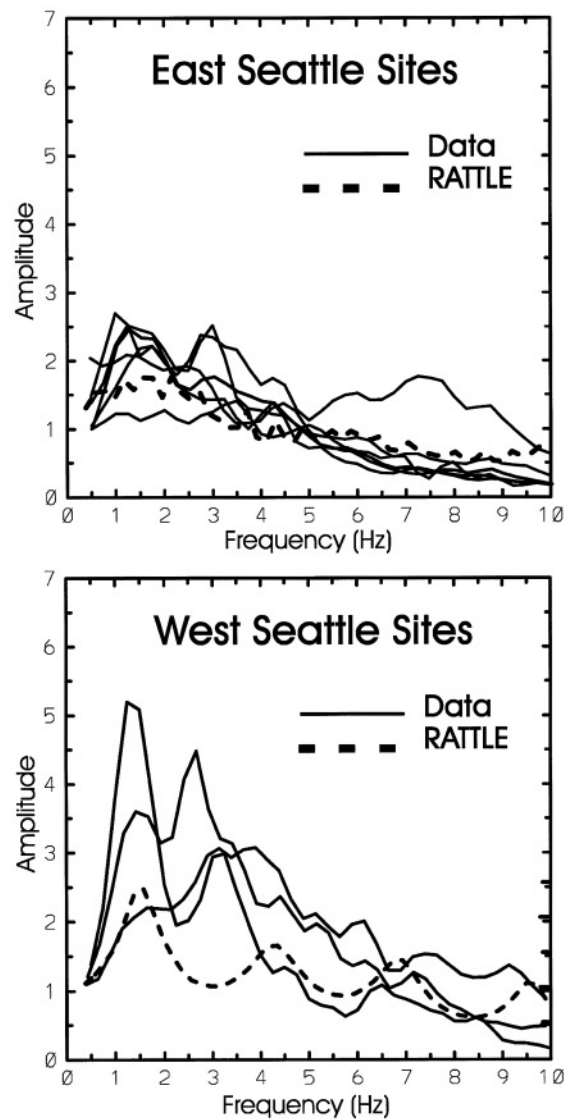


Figure 12. Comparison of site-response curves from earthquake data for sites on the hills east of downtown Seattle on till, and for sites in West Seattle with the predictions of the 1D SH velocity models in Tables 7 and 8.

plitudes. In east Seattle, the sequence is the same, except that it is capped with glacial till deposits and the depth to basement is much greater because this region overlies the Seattle basin (Yount *et al.*, 1985). Figure 1 shows the 500-m depth-to-basement contour from Yount *et al.* (1985). Our east Seattle 1D model has a gradient in shear-wave velocity in the nonglacial sediments down to bedrock. We calculate the predicted site amplification for a vertically propagating *S* wave through a stack of flat layers using the code RATTLE (C. S. Mueller, USGS, written comm., 1997). The results for east and west Seattle are shown overlaying the earthquake-data inversion response curves in Figure 12. The agreement

is fairly good for east Seattle till sites, but the theoretical response is about a factor of 2 lower than the observations for West Seattle.

We have also considered a 2D velocity model depicted in Figure 13, across West Seattle, Harbor Island, and the hills of east Seattle. This velocity profile is based on the geologic cross sections presented by Liesch *et al.* (1963) and the depth to basement map of Yount *et al.* (1985) with information on shallow velocity structure from the earlier 1D models. The cross section is meant to be representative of an east–west line near the latitude of the Seattle fault (Fig. 1). The finite-difference code of Frankel and Clayton (1986)

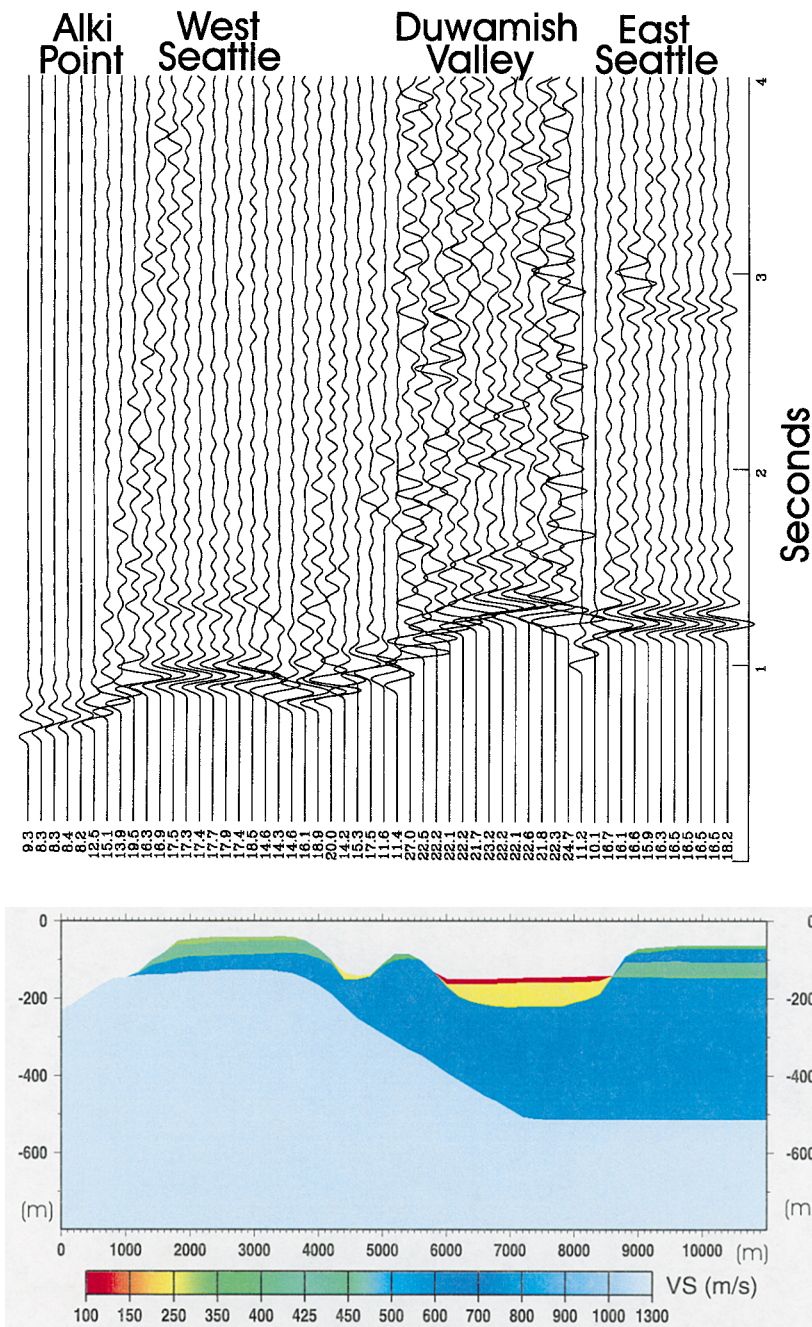


Figure 13. Relative ground-velocity synthetics from a 2D *SH* finite-difference calculation through an east-west velocity cross section near the latitude of the Seattle fault. Synthetics are lowpass-filtered at 10 Hz.

is used to calculate *SH* synthetics for a vertically traveling, horizontal-plane wave, input at the base of the model. The effect of topography is included by tapering the density to zero at the imposed free surface (Frankel and Leith, 1992). This technique was tested by comparison with the case of a horizontal free-surface boundary condition. A grid spacing of 1 m is used for a maximum frequency of accurate propagation of 10 Hz. The source is a Gaussian that appears as an approximate impulse below 10 Hz. The longer duration ground motion is apparent in the Duwamish Valley from the trapping of energy in low-velocity surface sediments. Figure 14(a) shows representative spectral ratios of the finite difference synthetics relative to Alki Point. As with the 1D modeling, theoretical amplification for east Seattle is close to the value obtained from earthquake data. The 2D model also yields amplification factors similar to 1D modeling and to the observations for fill sites of the Duwamish Valley. However, amplification in West Seattle is still about a factor of 2 less than observed. Figure 14(b) shows 3D-displacement response-spectral-intensity values for the finite-difference synthetics. Comparing these results with Figure 5, we see that the 2D calculation captures much of the ground-motion duration difference seen in the data.

Discussion and Conclusions

Simple spectral ratios and source–site inversion of ground-motion data from local earthquakes and the SHIPS experiment show amplifications between 3 and 4 below 5 Hz at West Seattle sites relative to Tertiary sandstone. Amplification factors for till sites on the hills of east Seattle average between 2 and 2.5 below 5 Hz. Amplification factors on artificial fill sites are about 30% higher on average than West Seattle sites. However, this measure of ground motion does not consider duration. When the duration of ground motion is included in a three-dimensional response-spectrum calculation, the 3D-displacement response-spectrum intensity is a factor of 2 to 3 greater on artificial fill than in West Seattle. Simple 1D and 2D *SH* models are able to predict observed amplification factors in east Seattle and the Duwamish Valley, but fall short of the observed amplification factors in West Seattle by a factor of 2. This discrepancy is most likely due to 3D effects. Our 2D cross section falls near the latitude of the Seattle fault. This fault dips to the south at approximately 20 degrees and has a thrust mechanism (Johnson *et al.*, 1994; Pratt *et al.*, 1997). North–south convergence along the Seattle fault has caused subsidence of the Seattle basin. The depth to basement and the thickness of nonglacial sedimentary deposits increases sharply moving from west to east and from south to north from our cross section, as seen in Figure 1. Frankel *et al.* (1999) have postulated the existence of basin-edge-induced surface waves in the West Seattle data. These arrivals are large dispersive phases following direct *S* caused by the conversion of *S* waves at the edge of the sedimentary basin. Langston and Lee (1983) and Ihnen and Hadley (1986) have also appealed

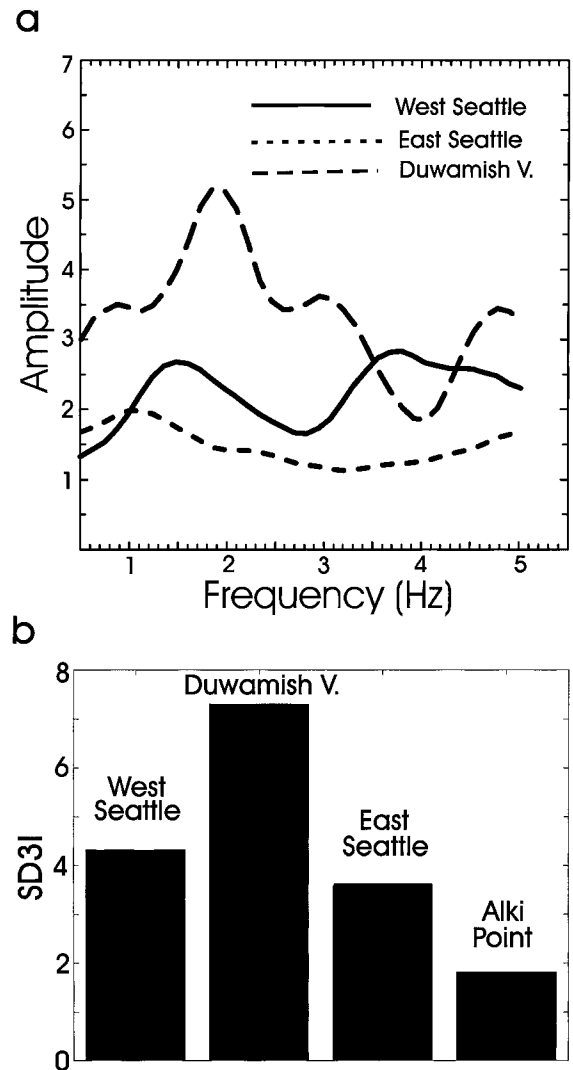


Figure 14. (a) Representative spectral ratios of the finite-difference synthetics in Figure 13. All ratios are referenced to the Alki Point synthetic. Amplification factors are consistent with the observations for east Seattle till sites and the Duwamish Valley fill sites. (b) 3D displacement-response spectral-intensity values for the same finite difference synthetics.

to focusing from 3D basin structures to explain the damage in West Seattle and the Duwamish Valley from the 1965 earthquake. The results of this study support the large site-response values obtained by Frankel *et al.* (1999) for West Seattle and come to the conclusion that these values are due to several different factors: lower impedance of the surficial glacial-outwash deposits, 3D basin-edge effects, and basin-geometry focusing effects.

Acknowledgments

The authors benefited from discussions with Rob Williams, Jack Odum, and Bill Stephenson. Susan Rhea provided GIS support.

References

- Anderson, J. G., and S. Hough (1984). A model for the shape of the Fourier amplitude spectrum of acceleration at high frequencies, *Bull. Seism. Soc. Am.* **74**, 1969–1994.
- Andrews, D. J. (1986). Objective determination of source parameters and similarity of earthquakes of different size, in *Earthquake Source Mechanics*, S. Das, J. Boatwright, and C. H. Scholz (Editors), American Geophysical Union, Washington, D.C., 259–268.
- Atkinson, G. M. (1995). Attenuation and source parameters of earthquakes in the Cascadia region, *Bull. Seism. Soc. Am.* **85**, 1327–1342.
- Bodin, P., and S. Horton (1999). Broadband microtremor observation of basin resonance in the Mississippi embayment, Central US, *Geophys. Res. Lett.* **26**, 903–906.
- Carver, D., and S. H. Hartzell (1996). Earthquake site response in Santa Cruz, California, *Bull. Seism. Soc. Am.* **86**, 55–65.
- Carver, D. L., K. W. King, R. A. Williams, and D. M. Worley (1998). Earthquake ground-response studies in West and South Seattle, Washington, in *Assessing Earthquake Hazards and Reducing Risk in the Pacific Northwest*, A. Rogers, T. Walsh, W. Kockelman, and G. Priest (Editors), *U.S. Geol. Surv. Profess. Pap. 1560*, 345–354.
- Dirlam, C. N. (1949). Reporting the Northwest earthquake—damage to buildings, *Building Standards Monthly* **18**, 4–7.
- Edwards, H. H. (1951). Lessons in structural safety learned from the 1949 Northwest earthquake, *Western Construction* **26**, 70–74.
- Field, E. H., and K. H. Jacob (1993). The theoretical response of sedimentary layers to ambient seismic noise, *Geophys. Res. Lett.* **20**, 2925–2928.
- Field, E. H., S. E. Hough, and K. H. Jacob (1990). Using microtremors to assess potential earthquake site response: a case study in flushing meadows, New York City, *Bull. Seism. Soc. Am.* **80**, 1456–1480.
- Field, E. H., A. C. Clement, K. H. Jacob, V. Aharonian, S. E. Hough, P. A. Friberg, T. O. Babiian, S. S. Karapetian, S. M. Hovanessian, and H. A. Abramian (1995). Earthquake site-response study in Giumri (formerly Leninakan), Armenia, using ambient noise observations, *Bull. Seism. Soc. Am.* **85**, 349–353.
- Fisher, M. A., T. Parsons, T. M. Brocher, R. D. Hyndman, A. M. Trehu, K. C. Creager, R. S. Crosson, N. P. Symons, T. L. Pratt, C. S. Weaver, Ten Brink (1999). Urban earthquake hazards of the Puget Sound region, initial findings from the 1998 SHIPS experiment, *Seism. Res. Lett.* **70**, 210.
- Frankel, A., and R. W. Clayton (1986). Finite difference simulations of seismic scattering: implications for the propagation of short-period seismic waves in the crust and models of crustal heterogeneity, *J. Geophys. Res.* **91**, 6465–6489.
- Frankel, A., and W. Leith (1992). Evaluation of topographic effects on *P* and *S*-waves of explosions at the northern Novaya Zemlya test site using 3-D numerical simulations, *Geophys. Res. Lett.* **19**, 1887–1890.
- Frankel, A., D. Carver, E. Cranswick, M. Meremonte, T. Bice, and D. Overturf (1999). Site response for Seattle and source parameters of earthquakes in the Puget Sound region, *Bull. Seism. Soc. Am.* **89**, 468–483.
- Galster, R. W., and W. T. Laprade (1991). Geology of Seattle, Washington, United States of America, *Bull. Assoc. Eng. Geol.* **28**, 235–302.
- Hartzell, S. H. (1992). Site response estimation from earthquake data, *Bull. Seism. Soc. Am.* **82**, 2308–2327.
- Hartzell, S., A. Leeds, A. Frankel, and J. Michael (1996). Site response of urban Los Angeles using aftershocks of the Northridge earthquake, *Bull. Seism. Soc. Am.* **86**, S168–S192.
- Hartzell, S., E. Cranswick, A. Frankel, D. Carver, and M. Meremonte (1997). Variability of site response in the Los Angeles urban area, *Bull. Seism. Soc. Am.* **87**, 1377–1400.
- Ihnen, S. M., and D. M. Hadley (1986). Prediction of strong ground motion in the Puget Sound region—the 1965 Seattle earthquake, *Bull. Seism. Soc. Am.* **76**, 905–922.
- Johnson, S. Y., C. J. Potter, and J. M. Armentrout (1994). Origin and evolution of the Seattle basin and Seattle fault, *Geology* **22**, 71–74.
- King, K. W., A. C. Tarr, D. L. Carver, R. A. Williams, and D. M. Worley (1988). Geophysical studies in support of seismic hazards assessment of Seattle and Olympia, Washington, *U.S. Geol. Surv. Open-File Rept.* 88-541.
- Langston, C. A., and J. J. Lee (1983). Effect of structure geometry on strong ground motion—the Duwamish River valley, Seattle, Washington, *Bull. Seism. Soc. Am.* **73**, 1851–1865.
- Liesch, B. A., C. E. Price, and K. L. Walters (1963). Geology and ground-water resources of northwestern King County, Washington, State of Washington Department of Conservation, Division of Water Resources, Water Supply Bulletin No. 20, 241 pp.
- Mullineaux, D. R., M. G. Bonilla, and J. Schlocker (1967). Relation of building damage to geology in Seattle, Washington during the April 1965 earthquake, *U.S. Geol. Surv. Profess. Pap. 575-D*, D183–D191.
- Nakamura, Y. (1989). A method for dynamic characteristics estimation of subsurface using microtremor on the ground surface, *Quarterly Report of the Railway Technical Research Institute* **30**, 1, 25–33.
- Olson, A. (1987). A Chebyshev condition for accelerating convergence of iterative backprojection methods—solving large least-squares problems, *Phys. Earth Planet. Interiors* **47**, 333–345.
- Pratt, T. L., S. Johnson, C. Potter, W. Stephenson, and C. Finn (1997). Seismic reflection images beneath Puget Sound, western Washington State: the Puget lowland thrust sheet hypothesis, *J. Geophys. Res.* **102**, 27469–27489.
- Safak, E. (1998). 3D response spectra: a method to include duration in response spectra, in *Proceedings of the Eleventh European Conference on Earthquake Engineering*, P. Bisch, P. Labbe, and A. Pecker (Editors), A. A. Balkema, Netherlands.
- Shannon and Wilson (1994). Kingdome seismic evaluation, Seattle, Washington, Report W-6836-01, Seattle, Washington, unpublished report.
- Waldron, H. H., B. A. Liesch, D. R. Mullineaux, and D. R. Crandell (1962). Preliminary geologic map of Seattle and vicinity, U.S. Geol. Surv. Map I-354.
- Weaver, C. S., K. G. Troost, D. B. Booth, A. Frankel, R. E. Wells, J. Mullen, and T. Nolan (1999). The Seattle urban seismic hazard mapping project: a USGS contribution to Seattle's project impact, *Seism. Res. Lett.* **70**, 256.
- Williams, R. A., W. J. Stephenson, A. D. Frankel, and J. K. Odum (1999a). Surface seismic measurements of near-surface *P*- and *S*-wave seismic velocities at earthquake recording stations, Seattle, Washington, *Earthquake Spectra* **15**, 565–584.
- Williams, R. A., W. J. Stephenson, J. K. Odum, and D. M. Worley (1999b). *S*-wave velocities for specific near-surface deposits in Seattle, Washington, *Seism. Res. Lett.* **70**, 257.
- Yount, J. C., G. R. Dembroff, and G. M. Barats (1985). Map showing depth to bedrock in the Seattle 30' by 60' quadrangle, Washington, U.S. Geol. Surv. Map MF-1692.

U.S. Geological Survey
 Denver Federal Center
 Box 25046 MS 966
 Denver, CO 80225

Manuscript received 3 February 2000.